Longitudinal Secretome Characterization of Renal Autologous Cell Therapy Candidate Rilparencel During Manufacturing

Ashley Greenawalt[1], Mark Rohlfing[1], Katherine James[1], Andrew Bruce[2], Dominic Justewicz[1]
[1]ProKidney, Bioanalytical Development, [2]ProKidney, Research & Development, Morrisville, NC, USA

INTRODUCTION

- Renal cell therapy has emerged as an investigational option to treat patients who have failed standard-of-care for chronic kidney disease (CKD).[1,2]
- The cells formulated in rilparencel are representative of the renal epithelial cell landscape of the nephron, derived from the proximal tubules through to the distal tubules/collecting ducts.[3]
- Here we provide comprehensive characterization of the distinct secretomic signatures of rilparencel cells during manufacture.

METHODS

- Rilparencel final product was manufactured for 6 patients in a Phase 2 investigative clinical trial of diabetes mellitus and stage 3-4 CKD (n=6, NCT05018416).
- Cryopreserved cells collected at four steps (T1, T2, T3, SRC) during manufacturing were incubated for 24 hours, and conditioned medium (CM) analyzed for >80 CKD-related secretory proteins[4-10] using commercial/custom test panels (Luminex xMAP Intelliflex). Selected renal cells (SRC) are final product. Analysis by Excel and R. Protein interaction network analysis (STRING v.12.5)[11,12] generated a proteomic landscape in manufacture.

RESULTS (Global Analysis)

Table 1: Secretome Testing Determination

Summary of Secretome Analysis[1]		
Parameter	**Positives[2]**	**Negatives[3]**
No. proteins	43	42

[1] Outcome of longitudinal testing using Intelliflex system, reported as pg/mL per 1K cells.
[2] Proteins detected (>LLOQ): A1M; Ang-2; ANGPTL-4, -6; β2M; calbindin; CD-54, -62P, -106, -137, -325 -365; clusterin; cystatin C; collagen IV α-1; GM-CSF; IL-1α, -4, -6, -8; MIP-1β; MCP-1; MMP-1, -2, -3, -7, -8, -9, -10; NAGLU; NGAL; OPN; procollagen 1 α-1; TGFβ-1, -2, -3;TIMP-1; TNFα; TNF-R1; uPAR; VEGF-A, -C.
Note: CD54 and MCP-1 were each detected in two separate kits.
[3] Proteins not detected (<LLOQ): Ang-1; BDNF; CD-31; DR-4, -5, -6; EGF; FGF-2; FST; GPNB; GSTA1; HGF; IFN-α, -γ; IL-10, -12p70, -13, -17A, -18, -22, -37; IP-10; MIP-1α; MMP-12, -13; NGF; PDGF; PIGF-1; RBP4; Renin; Resistin; SCF; TFF3; TNFRSF-5, -6, -7, -8, -14, -18; Umod; VEGF-D.

Statistical analysis of secretome between T1 & SRC (n=6):

- During the manufacturing of rilparencel, the secretome changes significantly between T1 and SRC.
- PERMANOVA p=0.031, R^2=0.47 (timepoint explains 47% of variation), PseudoF=8.75 (variation between timepoint > within), PERMDISP p=0.078 (similar within-group spread).

Abbreviations: PERMANOVA, permutational multivariate analysis of variance, PERMDISP, permutational multivariate analysis of dispersion.

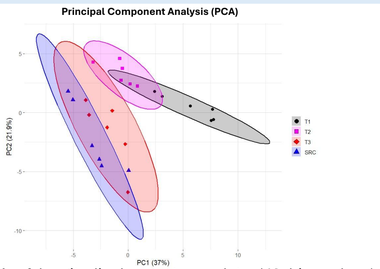

Figure 1: PCA of longitudinal secretome data (42 biomarkers) of clinical samples (n=6) show distinct clusters between time points (T1, T2, T3, SRC).

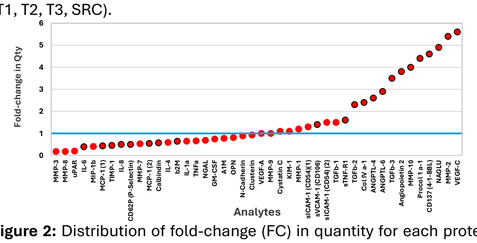

Figure 2: Distribution of fold-change (FC) in quantity for each protein (between SRC and T1). Blue line: FC threshold (1.0). Black outline (markers): 22 of 42 proteins across all 6 donors with p<0.05 per paired Wilcoxon test (Benjamini-Hochberg p-value 0.0597, lowest value possible due to dataset size).

RESULTS ('Inflammation Silencing')

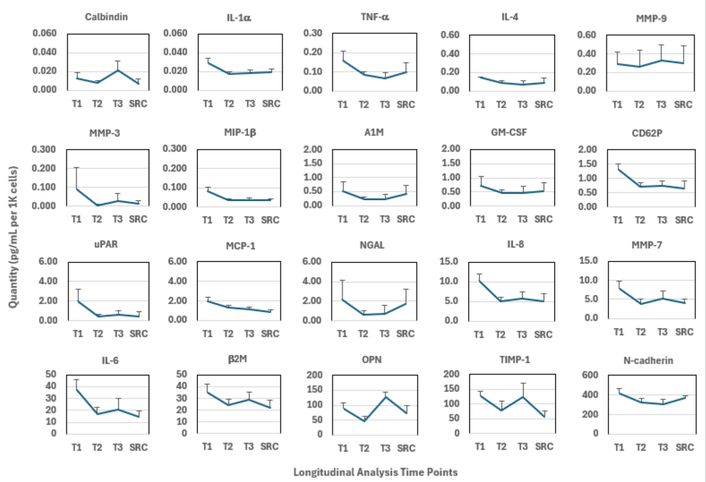

Figure 3: Highlighting 'inflammation silencing' factors decreasing during manufacture (FC <1.0). Mean +1 SD for simplicity of visualization. Note: MMP-8 not shown (~0.020 'Qty').

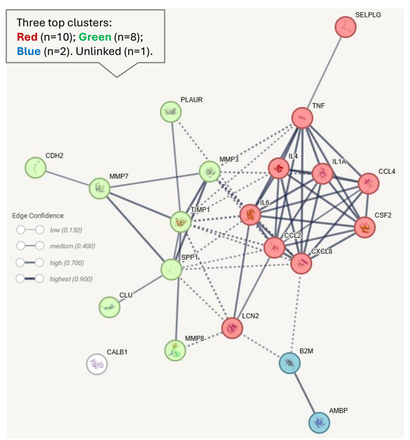

Figure 4: Clustering of STRING network for proteins comprising the 'inflammation silencing' secretome. The strength of the predicted protein associations (*i.e.*, 'nodes') is visualized by the thickness of the lines between nodes (*i.e.*, 'edges'), with the thickness indicating the confidence level: thickest with the highest (≥0.900), thinner with high (≥0.700), thinning with medium (≥0.400), and thinnest with lowest (≥0.150). The primary cluster incorporates half of the proteins, while three contain 95% at high confidence (≥0.700). The number of proteins (21 nodes) with interactions (61 edges) significantly exceed what would be expected for a random group.

Table 2: Top Functional Enrichment Terms for 'Inflammation Silencing' Secretome

Rank	Description	Count	Proteins	Signal	p-value (FDR)
WikiPathways					
1	Lung fibrosis	9 of 63	CCL-2, -4; GM-CSF; -4, -6, -8; OPN; TIMP-1	5.12	$1.52x10^{-14}$
2	Overview of proinflammatory and profibrotic mediators	10 of 126	CCL-2, -4; GM-CSF; IL-1α, -4, -6, -8; MMP3; OPN; TNF-α	4.40	$2.25x10^{-14}$
Tissue Expression (TISSUES)					
1	Inflammatory cell	6 of 14	CCL2; IL-1α, -4, -8; TNF-α	4.41	$6.19x10^{-11}$
Subcellular Localization(COMPARTMENTS)					
1	IL-12 complex	7 of 24	CCL2; GM-CSF; IL-1α, -4, -6, -8; TNF-α	4.98	$1.01x10^{-12}$
REACTOME Pathways					
1	IL-10 signaling	8 of 45	CCL-2, -4; IL-1α, -6, -8; GM-CSF; TIMP-1; TNF-α	4.76	$7.08x10^{-13}$
2	IL-4 & IL-13 signaling	9 of 107	CCL2; IL-1α, -4, -6, -8; NGAL; MMP-3; TIMP-1; TNF-α	4.00	$1.94x10^{-12}$
KEGG Pathways					
1	IL-17 signaling pathway	8 of 91	CCL2; GM-CSF; IL-4, -6, -8; MMP3; NGAL; TNF-α	3.78	$1.96x10^{-11}$
6	AGE-RAGE signaling pathway in diabetic complications	5 of 96	CCL2; IL-1α, -6, -8; TFN-α	1.97	$4.09x10^{-6}$

Abbreviations: FDR, false-discovery rate, or p-value (<0.05) of signal; KEGG, Kyoto encyclopedia of genes and genomes; STRING, search tool for the retrieval of interacting genes database.
Factors: CCL-2, chemokine ligand (C-C motif), or MCP-1, monocyte chemoattractant protein-1; CCL-4, or MIP-1β, macrophage inflammatory protein 1-β; GM-CSF, granulocyte macrophage colon-stimulating factor, or CSF2; IL-1α, interleukin-1α; IL-8, or chemokine ligand (C-X-C motif)-8; MMP-3, matrix metalloproteinase-3, or stromelysin-1; NGAL, neutrophil gelatinase-associated lipocalin; OPN, osteopontin; TIMP-1, tissue inhibitor of MMP 1; TNF-α, tumor necrosis factor-alpha.
Note: All protein-protein associations are annotated with confidence scores (pre-computed, with a scale between 0 and 1) that approximate the probability that a predicted link exists between two proteins in the same metabolic map in the KEGG database. Only confidence scores of ≥ 0.700 were used. STRING was applied to highlight protein-protein associations as it uniquely uses an unsupervised procedure to hierarchically predict its entire proteome-wide network into functional modules. The network generated incorporates functional, physical, and regulatory interactions between proteins. Enrichment analysis reports relevant metrics, primarily the enrichment signal, defined as a weighted harmonic mean between the ratio of observed to expected occurrences in an enriched term, and its p-value (FDR). Use of interaction and pathway knowledgebases provides insights into the functional context of individual proteins and understanding the biological organization of an entire protein dataset.
Also note: GO, KEGG, Reactome, and WikiPathways are each annotated knowledgebases and are integrated into the STRING platform as functional enrichment analysis categories to help connect protein interaction networks with annotated biological pathways. The primary strength of the annotated knowledgebases is their ability to contextualize high-throughput biological data by translating raw molecular lists into structural and functional biological insights. Protein interactions were predicted by STRING on the basis of evidence sources such as text mining, experimental evidence, databases, co-expression, neighborhood, and co-occurrence.

RESULTS ('Tissue Remodeling')

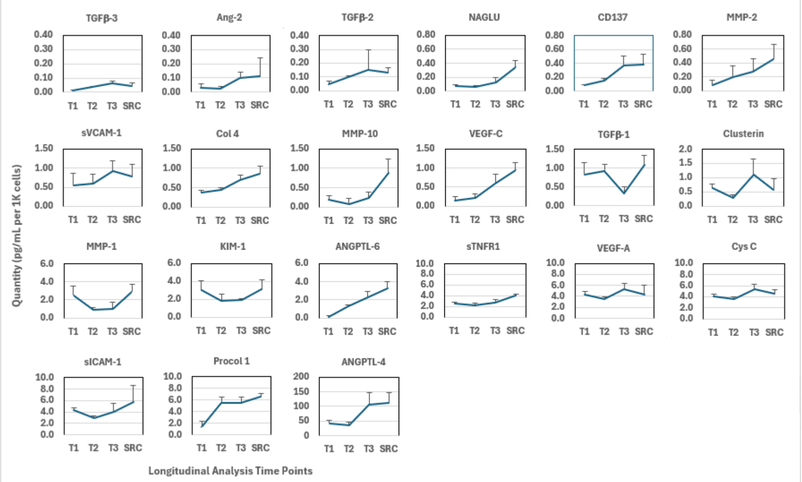

Figure 5: Highlighting 'tissue remodeling' factors increasing during manufacture (FC >1.0). Note: 95% of proteins with Qty < 10pg/mL per 1K cells (compared to 75% in Fig.3).

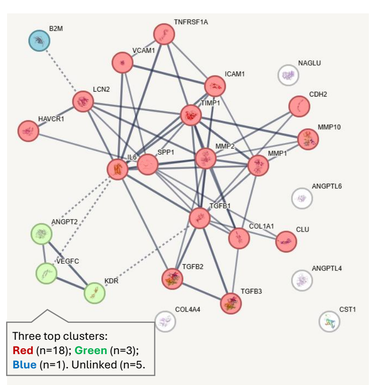

Figure 6: Clustering of STRING network for proteins of the 'tissue remodeling' secretome. This group of 27 proteins was selected to comprise proteins that increase in quantity during manufacturing (n=21, see Figure 5) and six with the overall highest quantity from secretome analysis and/or because of their reported renoprotective role (IL-6, β2M, OPN, TIMP-1, N-cadherin, and NGAL). The primary cluster incorporates two-thirds of the proteins, while three contain ≥80% at high confidence (≥0.700). The number of proteins (27 nodes) with interactions (58 edges) significantly exceed what would be expected for a random group.

Table 3: Top Functional Enrichment Terms for 'Tissue Remodeling' Secretome

Rank	Description	Count	Proteins	Signal	p-value (FDR)
Local Network Cluster (STRING)					
1	ECM organization	12 of 180	Col 1, 4; ICAM-1; MMP-1, -2, -10; OPN; TGFβ-1, -2, -3; TIMP-1	3.71	$3.58x10^{-14}$
2	Elastic fiber formation, and MMPs	8 of 61	MMP-1, -2, -10; OPN; TGFβ-1, -2, -3; TIMP-1	3.57	$7.10x10^{-11}$
WikiPathways					
2	Burn wound healing	9 of 100	Col 1; ICAM-1; IL-6; KDR; MMP-1, -2; TGFβ-2, -3; TIMP-1	3.51	$1.16x10^{-11}$
3	Photodynamic therapy-induced NF-kB survival signaling	6 of 34	ICAM-1; MMP-1, -2; VCAM-1	3.18	$3.51x10^{-9}$
KEGG Pathways					
3	Relaxin signaling pathway	6 of 126	Col 1, 4; MMP-1, -2; TGFβ-1; VEGF-C	1.82	$2.37x10^{-6}$
Biological Process (GO)					
1	Positive regulation of EMT	5 of 51	Col 4; IL-6; TGFβ-1, -2, -3	1.79	$1.69x10^{-5}$
3	Response to oxygen levels	9 of 318	Ang-2; ANGTPTL-4; Col 4; MMP-2; TGFβ-1, -2, -3; VEGF-C	1.50	$4.79x10^{-6}$

Abbreviations: ECM, extracellular matrix; EMT, epithelial-mesenchymal transition; FDR, false-discovery rate; GO, gene ontology database; STRING, search tool for the retrieval of interacting genes database.
Factors: Ang-2, angiopoietin-2; ANGPTL-4, angiopoietin-like protein-4; Col 1, procollagen 1α-1, type I; Col 4, collagen IV α-1, type IV; ICAM-1, inter-cellular adhesion molecule-1, or soluble CD54; IL-6, interleukin-6; KDR, kinase domain receptor, or VEGFR2, surrogate for VEGF-A; MMP-1, matrix metalloproteinase-1; OPN, osteopontin; TGFβ-1, transforming growth factor-β1; TIMP-1, tissue inhibitor of MMP type 1; TNFR1, tumor necrosis factor receptor 1; VCAM-1 (CD106), vascular cell adhesion molecule-1; VEGF-C, vascular endothelial growth factor-C.

RESULTS (Network Summary Features)

Table 4: Summary of STRING Network Analysis

Extent of Significant Enrichment				
Parameter	**'Inflammation Silencing'**	**'Tissue Remodeling'**	**Positives**	**Negatives**
Protein Interactions				
No. proteins	21	27	43	42
% proteins in 3 clusters (≥ 1)	95	80	77	80
No. edges (> random)	61	58	76	75
Avg. node degree (≥1.0)	5.80	4.30	3.30	3.75
Avg. local clustering coefficient (scale 0 to 1)	0.714	0.548	0.519	0.615
Functional Enrichment				
Top score (STRING signal)	5.12 (Lung Fibrosis)	3.71 (ECM Organization)	4.05 (Elastic Fiber Formation)	5.09 (Cytokine-cytokine Receptor Interactions)

Note: Functional enrichment analysis for the total number of positive (n=43, detected) and negative (n=42, not detected) factors in the samples is included here for comparison. Protein interaction scores for 'inflammation silencing' and 'tissue remodeling' indicate significant enrichment. Avg. node degree, avg. no. of interactions that each protein has in the network. Avg. local clustering coefficient, mean of local clustering coefficients of the network, measures how close a node's neighbors are to being fully connected to each other, thus ratio of existing edges between a node's neighbors divided by all possible edges.

LIMITATIONS

- The presentation focuses on clinical sample material (N=6) from Phase 2 NCT05018416, cohort 1, with half of the lots representative of the enrollment criteria and dosing regimen for the ongoing Phase 3 (NCT05099770 PROACT 1 trial).
- For this study, cells were collected at four stages of rilparencel manufacturing and cultured for 24 hours. Reported results represent proteins secreted in an *in vitro* environment.

SUMMARY AND CONCLUSIONS

- The PCA plot **(Figure 1)** demonstrates distinct clusters at each time point during manufacture suggesting that the rilparencel secretome can be characterized as a unique signature dependent on the manufacturing step.
- Secretome analysis **(Table 1, Figures 2, 3, 5)** presents an argument that manufacturing progression reduces a pro-inflammatory output in favor of an increase of potential renoprotective ECM-remodeling capacity.
- Proteomic analysis **(Figures 4 and 6, Tables 2 to 4)** provides insights into the altered proteomic landscape during manufacturing progression.

REFERENCES

1. Cizman B, Butler EL, Stavas J, *et al.* A randomized clinical trial of kidney autologous cell therapy in diabetic kidney disease. *Clin J Am Soc Nephrol* 2026; 21:744-753.
2. Rossing P. Cell therapy: The next frontier in CKD management. *Clin J Am Soc Nephrol* 2026; 21:733-734.
3. James K, Greenawalt A, Rohlfing M *et al.* Cell-specific inflammatory profile characterization of the cell therapy candidate rilparencel. *J Am Soc Nephrol* 2025; doi:10.1681/ASN. 2025brzws2h8.
4. Greenawalt A, Rohlfing M, Bauer B, *et al.* Phase 3 clinical candidate rilparencel demonstrates distinct secretomic signatures at key points in manufacturing, suggesting a reduced inflammatory and fibrotic profile. *J Am Soc Nephrol* 2024; doi:10.1681/ASN.20244hqkbsr9.
5. Van Nynatten LR, Miller MR, Patel MA, *et al.* A novel multiplex biomarker panel for profiling human acute and chronic kidney disease. *Sci Rep* 2023;ddoi:10.1038/ s41598-023-47418-9.
6. Li Z-L, Li X-Y, Zhou Y, *et al.* Renal tubular epithelial cells response to injury in acute kidney injury. *eBioMed* 2024; doi:1016/j.ebiom.2024.105294.
7. Sadasivam M, Jie C, Hamad ARA. Renal tubular epithelial cells are constitutive non-cognate stimulators of resident T cells. *Cell Rep 2023;* doi:1016/j.celrep.2023.113210.
8. Scheidereit EM, Mavrommatis L, Kuppe C. Cell-cell crosstalk in kidney health and disease. *Nat Rev Nephrol* 2026; doi:1038/s41581-025-010125-1.
9. Gu C, Shi X, Dang X, *et al.* Identification of common genes and pathways in eight fibrosis diseases. *Front Genet* 2021; doi:10.3389/fgene.2020.627396.
10. Ding DY, Bot VA, Chen KL, *et al.* Plasma proteomic signatures of cellular aging predict human disease. *Nat Med* 2026; 32:2060-2072.
11. Szklarczyk D, Nastou K, Koutrouli M, *et al.* The STRING database in 2025: Protein networks with directionality of regulation. *Nucl Acids Res* 2025; 53:D730-D737.
12. Hong S-Y, Qin B-L. The altered proteomic landscape in renal tubular epithelial cells under high oxalate stimulation. *Biology* 2024; doi:3390/biology13100814.

ACKNOWLEDGEMENTS

- Eric Labonté, PhD, R&D ProKidney, for helpful discussions on data interpretation.

POSTER CONTACT

- Dominic Justewicz, PhD | dominic.justewicz@prokidney.com

Presented at ASN Kidney Week; October 22nd - 25th 2026, Denver CO.

Scan to Download